Protein Science (2000), *9*:2427–2435. Cambridge University Press. Printed in the USA.

Fibers of tau fragments, but not full length tau, exhibit a cross β-structure: Implications for the formation of paired helical filaments

A.M. GIANNETTI,[1] G. LINDWALL,[2,3] M.-F. CHAU,[3] M.J. RADEKE,[3] S.C. FEINSTEIN,[3,4] AND L.A. KOHLSTAEDT[2,3]

[1]Program in Biochemistry, California Institute of Technology, University of California, Santa Barbara, California 93106
[2]Department of Chemistry and Biochemistry, University of California, Santa Barbara, California 93106
[3]Neuroscience Research Institute, University of California, Santa Barbara, California 93106
[4]Department of Molecular Cellular and Developmental Biology, University of California, Santa Barbara, California 93106

(RECEIVED June 29, 2000; FINAL REVISION September 18, 2000; ACCEPTED September 18, 2000)

Abstract

We have used X-ray fiber diffraction to probe the structure of fibers of tau and tau fragments. Fibers of fragments from the microtubule binding domain had a cross β-structure that closely resembles that reported both for neurofibrillary tangles found in Alzheimer's disease brain and for fibrous lesions from other protein folding diseases. In contrast, fibers of full-length tau had a different, more complex structure. Despite major differences at the molecular level, all fiber types exhibited very similar morphology by electron microscopy. These results have a number of implications for understanding the etiology of Alzheimer's and other tauopathic diseases. The morphology of the peptide fibers suggests that the region in tau corresponding to the peptides plays a critical role in the nucleation of fiber assembly. The dramatically different structure of the full length tau fibers suggests that some region in tau has enough inherent structure to interfere with the formation of cross β-fibers. Additionally, the similar appearance by electron microscopy of fibrils with varying molecular structure suggests that different molecular arrangements may exist in other samples of fibers formed from tau.

Keywords: aging; Alzheimer's disease; amyloid; fiber diffraction; neurodegeneration; neurofibrillary tangles; paired helical filaments; tau

Tau, discovered as copurifying with tubulin (Weingarten et al., 1975), is abundant in nerve cell axons where it establishes cell polarity (Caceres & Kosik, 1990) and stabilizes microtubule dynamics (Binder et al., 1985; Drechsel et al., 1992; Panda et al., 1995; Black et al., 1996). It remains soluble when boiled (Fellous et al., 1976; Cleveland et al., 1977a) or exposed to acid (Lindwall & Cole, 1984), treatments that precipitate most proteins. In marked contrast, tau in neurofibrillary tangles (NFTs) forms a highly insoluble aggregate that is a hallmark pathology of Alzheimer's disease (Brion et al., 1985; Grundke-Iqbal et al., 1986; Kosik et al., 1986; Wood et al., 1986; Goedert et al., 1988; Wischik et al., 1988a). NFTs are composed of paired helical filaments (PHFs). Similar PHFs, also composed of tau, are found in other neurological disorders (Feany & Dickson, 1996; Trojanowski & Lee, 1998), including cases where there is a direct genetic link between tau mutations and disease (Hutton et al., 1998; Spillantini et al., 1998).

Alzheimer's disease PHFs visualized by electron microscopy usually have a twisted, right-handed morphology with a helical repeat of about 80 nm and a width of 12–20 nm, although the exact morphology depends on preparation methods (Crowther & Wischik, 1985; Wischik et al., 1985; Ruben et al., 1992; Feany & Dickson, 1996). Fibers produced in vitro are similar (Crowther et al., 1992, 1994; Goedert et al., 1996a). Tau fibers formed in other neurodegenerative diseases are also similar, although each has distinct characteristics (Feany & Dickson, 1996).

There are six tau isoforms generated by differential splicing. Tau can have either three or four 18 amino acid microtubule binding repeats separated from one another by inter-repeat regions of 13 or 14 amino acids (Fig. 1) (Goedert et al., 1988; Lee et al., 1988). Each of these two C-terminal splicing variants can have any of three N-terminal splicing variations (Kosik et al., 1989). PHFs exhibit a protease resistant core (Wischik et al., 1988a, 1988b). The core is composed primarily of the microtubule binding repeats, but encompasses only three repeats (Jakes et al., 1991; Green-

Reprint requests to: L.A. Kohlstaedt, Department of Chemistry and Biochemistry, University of California, Santa Barbara, Santa Barbara, California 93106; e-mail: kohlstaedt@chem.ucsb.edu.

Abbreviations and symbols: 3R tau, tau isoform without exon 10, containing only three repeats; 4R tau, tau isoform with four sequence repeats in the microtubule binding region; HEPES, *N*-(2-hydroxyethyl)piperazine-*N′*-(2-ethane sulfonic acid); tris, tris-(hydroxymethyl) amino methane; HPLC, high-pressure liquid chromatography; IPTG, isopropylthiogalactoside; MAP, microtubule associated protein; NFT, neurofibrillary tangle; PHF, paired helical filament; SDS, sodium dodecyl sulfate.

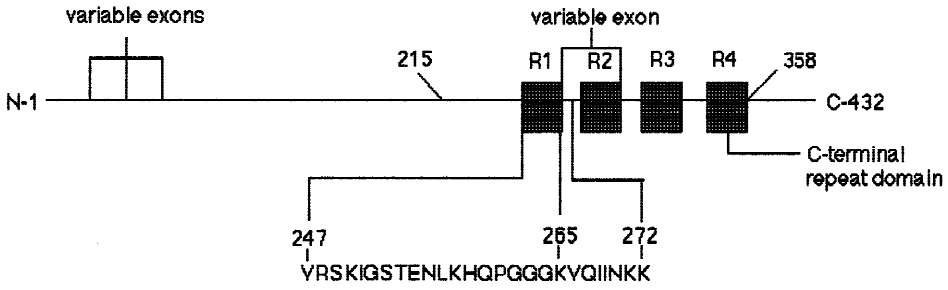

Fig. 1. Schematic diagram showing the structural features of tau known from its primary sequence. Six splicing isoforms are generated by the variable presence of two N-terminal exons and one C-terminal exon. Tubulin binding repeat sequences are shown as shaded boxes. Isoforms that contain the variable C-terminal exon (exon 10) are called 4R taus; isoforms lacking this exon are 3R taus. Fibers suitable for X-ray diffraction were obtained from two peptides whose sequences are indicated, from the entire region containing the four microtubule binding repeats, and also from full length 4R tau containing all three variable exons.

berg et al., 1992; Ksiezak-Reding et al., 1995; Goedert et al., 1996a), although all six isoforms have been recovered from dispersed PHFs (reviewed in Goedert et al., 1996b).

A key to treatment and prevention of tauopathic diseases lies in understanding PHF structure. Although fibers rarely form crystals, fiber diffraction allows us to explore molecular structure to a limited extent. We have collected diffraction patterns of fibers grown from the microtubule binding domain of tau, from each of two peptides corresponding to small fragments from within the microtubule binding domain, and also from fibers formed from the longest tau isoform, 4R tau. Fibers of the binding domain and the two peptides exhibit a cross β-diffraction pattern. In contrast, fibers of 4R tau have a significantly different diffraction pattern. Our results support the notion that PHFs are cross β-fibrils and suggest that small regions from the microtubule binding domain are sufficient to form fibrils with the properties of PHFs. Nevertheless, at least one tau isoform can form significantly different fibers. These data raise the possibility that not all fibers formed from tau or tau peptides have the same molecular structure. Further, our results are consistent with a model where sequences outside of the microtubule binding region have structural influences upon the microtubule binding domain (Goode et al., 1997), with this influence carrying over to affect the nature of the fibers formed from tau.

Results

Diffraction patterns of tau and tau peptide fibers

To understand the formation of tau fibers in neurodegenerative diseases, we compared the physical properties of full-length tau to tau fragments that are known to be present within the PHF core (Kondo et al., 1988; Brion et al., 1991a; Ksiezak-Reding & Yen, 1991; Novak et al., 1993) as well as to retain microtubule binding activity (Ennulat et al., 1989; Lee et al., 1989; Butner & Kirschner, 1991; Goode & Feinstein, 1994; Gustke et al., 1994). We have grown fibers in vitro of the longest isoform of rat central nervous system tau, 4R tau, which contains all three developmentally regulated exons. We have also grown fibers of the domain spanning amino acids 215–358, which contains tau's entire microtubule binding repeat region, and we have grown fibers of two small peptides from the repeat region (Fig. 1). The smallest peptide corresponds to amino acids 265–272 (KVQIINKK), the "interrepeat" region between repeats 1 and 2. 265–272 is removed by splicing in three repeat (3R) tau, but is the region that contributes the most to microtubule binding in 4R tau (Goode & Feinstein, 1994). The larger peptide extends from amino acids 247–272 (VRSKIGSTEN LKHQPGGGKVQIINKK). It includes the first repeat and interrepeat region.

We grew all fibers by vapor diffusion. In three cases, the largest fiber aggregates obtained were approximately $0.5 \times 0.25 \times 0.25$ mm (Fig. 2). These macroscopic fibers were birefringent but nonextinguishing, with parallel striations visible under polarized light running parallel to the long axis of the object. The only fiber of $tau_{247–272}$ that was large enough for diffraction analysis has a spiral morphology. The only large fiber of the microtubule binding domain, $tau_{215–358}$, was 0.8 mm in diameter and had a slightly different gross morphology than the other fibers. It was macroscopically twisted so that it appeared nearly spherical, as if it were rolled up like a ball of yarn. All the fibers exhibited many of the physical characteristics of protein crystals, including shattering when crushed. Drops often also contained a large number of smaller aggregates still visible by light microscopy whose fibrous nature was obvious (Fig. 2A). The largest fibers were mounted in glass capillaries bathed in a vapor of mother liquor and used for fiber diffraction analysis.

Figure 3A shows the diffraction pattern for the $tau_{265–272}$. Although only eight amino acids long, this peptide retains the ability to assemble microtubules, unlike peptides of the same composition but of scrambled sequence (Goode & Feinstein, 1994). A strong reflection on the meridian at 4.7 Å is diagnostic for a cross β-fibril (Pauling & Corey, 1951) (for an excellent review, see Dickerson, 1964). Cross β-fibers are made up of β-sheets packed with the direction of the β-strands perpendicular to the fiber axis. The $tau_{265–272}$ pattern has the 4.7 Å meridional reflection split into four very strong reflections representing distances from 4.56 to 4.79 Å. These reflections can be indexed as layer lines 48–51, giving a calculated repeat of 232 Å (Table 1). This repeat is slightly more than twice the length calculated for a number of other types of amyloid fibrils (Blake & Serpell, 1996; Sunde et al., 1997). The structural difference, however, can be interpreted as a slight change in pitch. Other amyloid fibrils have been modeled as a continuous beta sheet having 24 β-strands in a 115.5 Å repeat distance. Each β-strand is twisted by 15° to complete one turn in the 115.5 Å distance. The $tau_{265–272}$ peptide fibril would simply have to be underwound by slightly more than 0.3° per β-strand (each strand twisted by about 14.69°) to fit the same model, leading to an

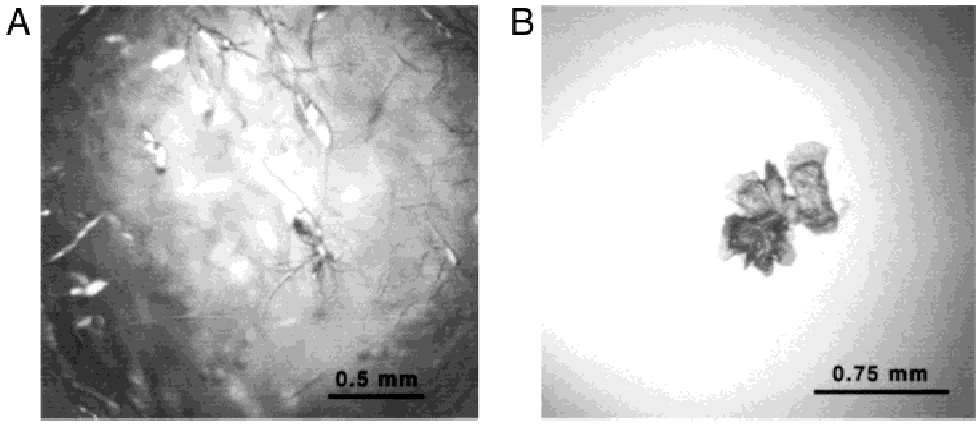

Fig. 2. Examples of macroscopic tau fibers in situ in the hanging drops of vapor diffusion experiments. **A:** Fibers of the $tau_{265–272}$. This drop contained both large fibers suitable for X-ray diffraction and a large number of smaller, but still macroscopic fibers. **B:** Fibers of full-length 4R tau. The fibers from this clump were separated to yield several individual fibers large enough for X-ray diffraction. Under polarized light each fiber showed striations running parallel to the long axis of the object.

approximate repeat of 49 strands. $Tau_{265–272}$ fibers have a large number of equatorial reflections corresponding to radial electron density (Table 2). Conspicuously absent is a strong reflection at 10 Å, which has been interpreted as arising from the packing of β-sheets against each other. Unlike the well-studied fibers formed by silk (Marsh et al., 1955), the side chain sizes on the peptide cover a broad range. Because no single low-angle reflection on the equator is unusually strong, the intersheet distance apparently has a range of packings that are all accommodated in the gross structure of the fiber. $Tau_{265–272}$ fibers do exhibit a weak reflection at both 10.6 and 10.7 Å. Cross β-fibers formed from a variety of other amyloidogenic proteins also lack a strong reflection at 10 Å (Sunde et al., 1997). The best fit found for indexing the equatorial reflections (Table 2) gives a "unit cell" dimension of 148 Å, suggesting an upper limit for the total diameter of a superhelically wound fibril. This width for a unit fibril is in agreement with the width (12–15 nm [120–150 Å]) seen for the narrowest fibers in these samples by electron microscopy (see below).

$Tau_{247–272}$ formed macroscopically twisted fibers with a corkscrew-like morphology (not shown). Due to their morphology, the $tau_{247–272}$ fiber diffraction pattern was cylindrically averaged perpendicular to the fiber axis. The most prominent feature, however, was a single sharp circular transform at 4.7 Å, suggesting that these fibers also have a cross β-morphology. $Tau_{247–272}$ fibers exhibited no other reflections of comparable intensity and showed none of the transforms that are prominent in the pattern of 4R tau (see below). $Tau_{215–358}$ fibers formed a macroscopic mass that was nearly spherical and exhibited a circular pattern of birefringence. Their fiber diffraction pattern also showed circular disorder, with a broad maximum between 4.78 and 4.65 Å as its only feature (Fig. 3B). Longer X-ray exposure did not reveal any additional reflections.

Figure 3C shows the diffraction pattern obtained for 4R tau fibers. These fibers exhibit some semicrystalline features. There are a number of lattice transforms convoluted with the fiber pattern, at least some of which can be accounted for in a crude model of the fiber (see below). Although these spots could also arise from a contaminating salt, the fibers were grown in a low salt solution and were never allowed to dry. The fiber pattern also has a large

Table 1. *Meridional reflections for $tau_{265–272}$*

Index	Spacing (Å)	Calculated repeat (Å)[a]
48	4.79	230.1
49	4.73	231.8
50	4.65	232.7
51	4.56	232.5

[a]The mean repeat distance is 231.8 Å.

Table 2. *Equatorial reflections for $tau_{265–272}$*

Index	Resolution observed (Å)[a]	Resolution calculated (Å)	d calc (Å)[b]
6	24.8, 24.2, 24.50	24.67	147.00
8	18.7, 18.2, 18.45	18.51	147.60
13	11.3, 11.1, 11.20	11.39	145.60
14	10.7, 10.6, 10.65	10.57	149.10
16	9.3, 9.2, 9.25	9.25	148.00
17	8.80, 8.74, 8.77	8.71	149.09
18	8.10, —, 8.10	8.22	145.80
19	7.87, 7.78, 7.83	7.79	146.68
20	7.50, 7.42, 7.46	7.40	149.20
21	7.00, 6.90, 6.95	7.05	145.95
23	6.50, 6.40, 6.45	6.44	148.35
24	6.20, 6.10, 6.15	6.17	147.60
26	5.75, 5.70, 5.73	5.69	148.85
27	5.60, 5.60, 5.60	5.48	151.20
29	5.15, 5.10, 5.13	5.10	148.63
Average packing distance			148.04

[a]Observed resolution for the left and right sides of the pattern and their average.

[b]Calculated "unit cell" or packing distance between centers of fibrils. Calculations and indexing were done as described by Burge (1963).

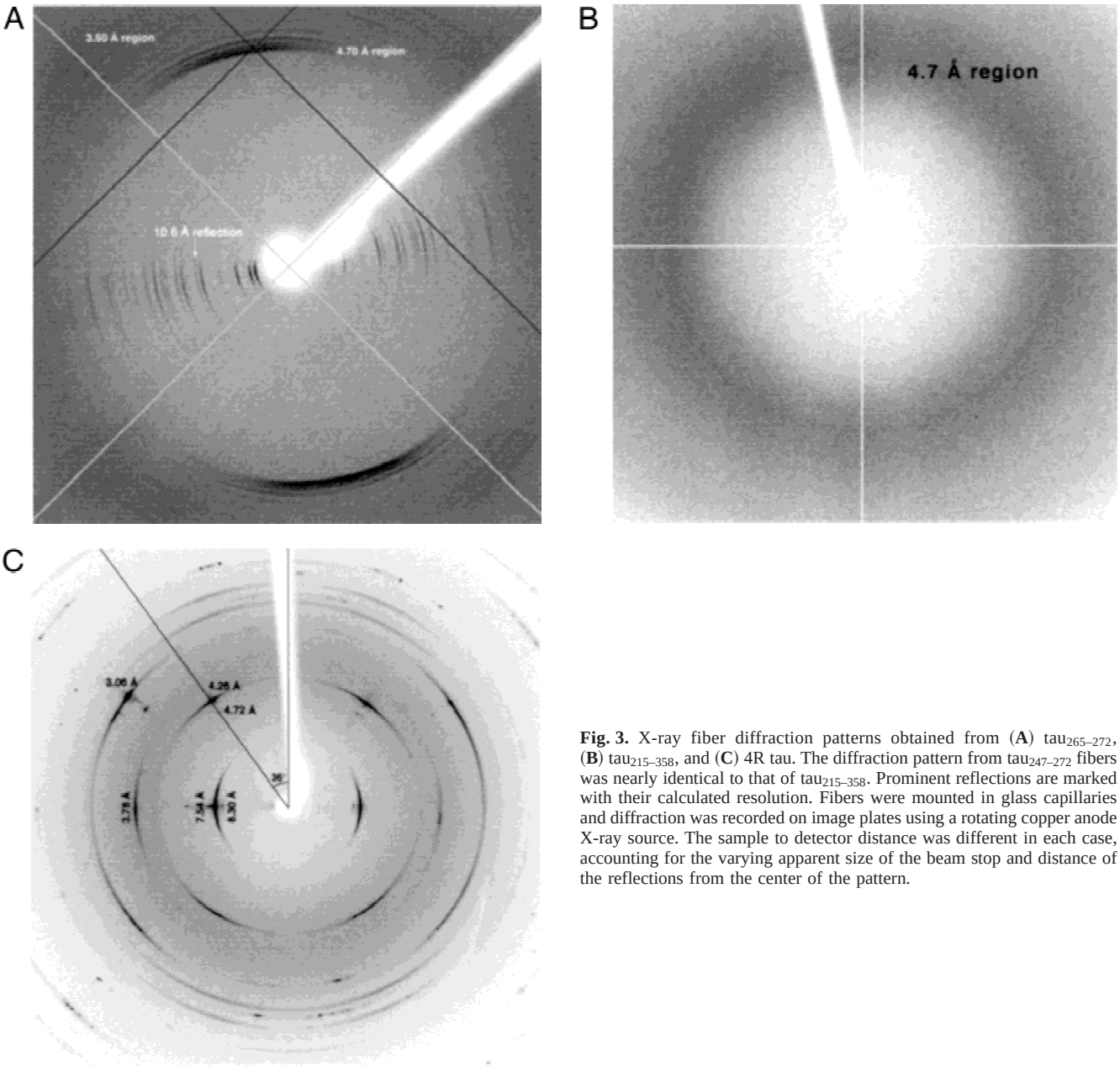

Fig. 3. X-ray fiber diffraction patterns obtained from (**A**) $tau_{265–272}$, (**B**) $tau_{215–358}$, and (**C**) 4R tau. The diffraction pattern from $tau_{247–272}$ fibers was nearly identical to that of $tau_{215–358}$. Prominent reflections are marked with their calculated resolution. Fibers were mounted in glass capillaries and diffraction was recorded on image plates using a rotating copper anode X-ray source. The sample to detector distance was different in each case, accounting for the varying apparent size of the beam stop and distance of the reflections from the center of the pattern.

number of off-meridional reflections. Although knowing the diffraction pattern to higher resolution might resolve the matter, these reflections could arise from the coexistence of a mosaic of different helical packings. This combination of semicrystalline order with mosaicity of packing makes the assignment of layer lines difficult. Strong reflections on the equator are at 3.78 and 7.54 Å. There is no arc on the meridian at 4.7 Å. One of the off meridional reflections is a very strong transform at 4.26 Å tilted 36° away from the meridian. At the same angle relative to the meridian is a faint 4.7 Å transform.

The 4R tau fiber pattern is too complex to allow inference of the general features of the structure(s) it represents. It is possible, however, to exclude some types of fiber structures and to guess at some possible components of the fiber composition. Because there is no reflection on the meridian at 4.7 Å, β-strands perpendicular to the fiber axis are not a prominent feature, and this diffraction pattern cannot be fit to a cross β-fiber model.

The reflection at 4.26 Å can be interpreted as a sign of β-structure aligned neither perpendicular nor parallel to the fiber axis. Starting from the parallel conformation, a β-sheet tilted around the fiber axis by 27° and around the axis of the incident X-ray beam by 36° would give such a reflection because the interstrand distance would be seen in projection in the fiber pattern. Rotation of the sheet about the fiber axis will periodically bring the full 4.7 Å spacing into a diffracting position, yielding the weak 4.7 Å transform at the same angle from the meridian as the 4.26 Å arc. Strong equatorial reflections could represent major pseudo-repeat distances within the tilted β-sheet. Alternately, strong reflections on the equator at 7.5 and 3.25 Å could indicate close packing of an α-helical component along the fiber axis.

Appearance of fibers by electron microscopy

We removed the mother liquor surrounding the macroscopic fibers and investigated its contents by electron microscopy (Fig. 4). Both of the peptides and full-length 4R tau formed filaments that resemble the filaments seen in brain tissue from Alzheimer's disease and other dementias. The mother liquor from $tau_{215–358}$ fibers became opaque when dried on electron microscope grids and could not be investigated. Thick bundles of fibers were common in the three samples examined, as would be expected because macroscopic bundles were removed from the same drops. These bundles ranged widely in size from 25 nm to several hundred nm in diameter. They all appeared to be assembled from smaller fibers. The smallest fibers seen, presumably single fibers, were 12–15 nm [120–150 Å] wide, a width similar to filaments seen in various neurodegenerative diseases. This was true for all three fiber types, although unit fibers were very rare for $tau_{247–272}$. Unit fibers are marked with arrows in Figure 4. It is noteworthy that the unit fibers were all similar in width and appearance despite the 50-fold difference in size between 4R tau and $tau_{265–272}$.

Unit fibers of all three fiber types bear a resemblance to the tau filaments found in Alzheimer's disease and in tauopathies. They show a longitudinally striped ribbon, with two pale stripes flanked by shadowed areas in the middle and at the edges, giving the appearance of paired fibers. In all cases, however, the typical helical pitch found in Alzheimer's disease PHFs is absent. The single and aggregate fibers of $tau_{265–272}$ consistently appear to have neatly parallel stripes while the stripes on 4R tau and $tau_{247–272}$ are less perfectly aligned. $Tau_{265–272}$ fibers were generally quite straight; fibers of the other two peptides were generally curved rather than straight. Thus, the fibers of $tau_{265–272}$ seem more stiff and less prone to twisting and bending than the fibers from the larger molecules. $Tau_{265–272}$ fibers were consistently slightly darker than the other fiber types, indicating either a denser structure or increased binding of the uranyl acetate stain. The morphologies of the different fibers are otherwise similar by electron microscopy.

The greatest difference between the fibers we have grown and PHFs seen in Alzheimer's disease brain is the lack of apparent helical character. In previous reports of PHF-like fibers grown in vitro from tau (Montejo de Garcini et al., 1988; Crowther et al., 1994) or tau fragments (Crowther et al., 1992; Schweers et al., 1995; Pérez et al., 1996; Yanagawa et al., 1998; von Bergen et al., 2000), the fibers have been visualized by electron microscopy. These fibers may or may not be helical, but generally resemble the unit fibers that we have observed. Large fiber bundles similar to those reported here have been grown in the presence of heparin (Pérez et al., 1996). The helical character of fibers is easily changed by details of preparation and handling. For instance, treatment of PHFs with NaOH causes them to lose their helicity (Wischik et al., 1985). Heparinase treatment also disrupts the helical character of PHFs (Arrasate et al., 1997), whereas heparin promotes formation of helical filaments in three repeat tau (Goedert et al., 1996a). By contrast, four repeat tau treated with heparin forms straight filaments (Goedert et al., 1996a).

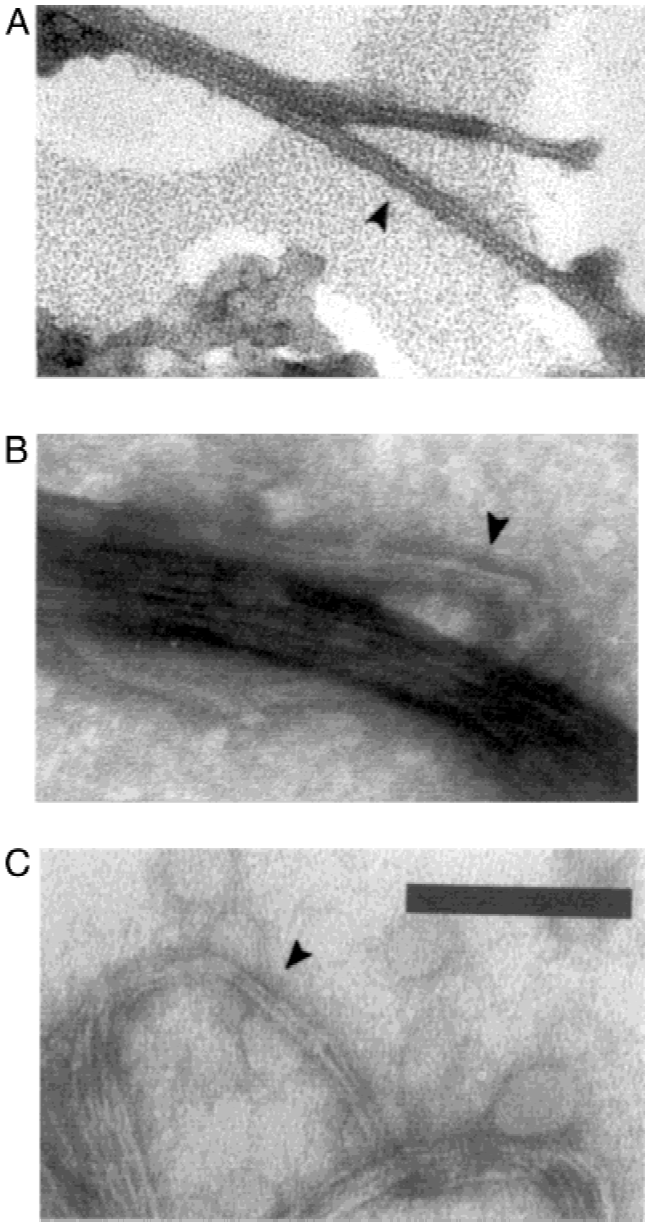

Fig. 4. Electron micrographs of fibers present in the mother liquor from which macroscopic fibers had been harvested for X-ray diffraction. (**A**) $tau_{265–272}$, (**B**) $tau_{247–272}$, (**C**) 4R tau. All are shown at the same magnification. Presumed unit fibers are marked with arrows. Scale bar = 100 nm. In (**A**), individual filaments can be seen separating at one end from a bundle of filaments. Single filaments of $tau_{265–272}$ averaged 13.3 ± 1.5 nm, $n = 8$. In **B** and **C**, a single fiber loops around a wider fiber bundle typical of those seen in all three cases. Only two unit fibers were found in $tau_{247–272}$ fiber samples. The two examples measured 15.1 and 14.4 nm, respectively. Single 4R fibers averaged 11.8 ± 1.1 nm, $n = 7$. $Tau_{265–272}$ fibers consistently stained somewhat darker than the others, which makes its unit fibers appear thinner. Fiber widths were measured directly off the 2.5 × 3 in. negative with the aid of a micrometer. All photographed examples were measured in each case, and the results were averaged.

Content of the macroscopic fiber aggregates

After diffraction analysis, macroscopic fibers of both 4R tau and $tau_{215–358}$ were washed, dissolved, and analyzed by SDS polyacrylamide gel electrophoresis. Unlike authentic PHFs, the fibers dissolved easily. Only a single band, of the same size as the starting material, was seen. The microscopic fibers observed by electron microscopy were taken from the same drops that contained undegraded macroscopic fibers.

Discussion

A common thread among many neurodegenerative diseases, ranging from dementias with a clearly genetic nature (Reed et al., 1997; Spillantini et al., 1997; Hutton et al., 1998; Spillantini et al., 1998) to injury-driven dementia pugilistica (Bouras et al., 1997), is the formation of pathological fibers composed of tau. We have grown fibers of 4R tau and three shorter fragments, all of which possess microtubule binding and assembly activities (Goode & Feinstein, 1994; Panda et al., 1995; Goode et al., 1997). In fact, the eight amino acid peptide $tau_{265–272}$ (KVQIINKK) is the region of tau with the most potent microtubule binding activity; this effect is specific because the scrambled amino acid sequence loses all tubulin binding affinity (Goode & Feinstein, 1994).

Nature of the fibers in protein folding diseases

The deposition of amyloid fibers is a key characteristic of protein folding diseases. These diseases include the spongiform encephalopathies (prion proteins), systemic amyloidoses (serum amyloid A, lysozyme, insulin), familial amyloid polyneuropathies (transthyretin, apolipoprotein A-1), amyotrophic lateral sclerosis (superoxide dismutase) and Alzheimer's disease (β-amyloid protein, tau) (for review, see Kelly, 1996). The pathological fibers are composed of a wide array of precursor proteins that, in their nonpathological native folds, occupy many different biochemical niches. These precursors bear no structural resemblance to one another. While the mechanisms of fiber formation in most protein folding diseases are poorly understood, the fibril has been found to possess a cross β-structure in each case in which structure has been assessed by diffraction analysis (Pauling & Corey, 1951; Dickerson, 1964; Eanes & Glenner, 1968; Booth et al., 1997; Inouye & Kirschner, 1997; Malinchik et al., 1998). Cross β-fibrils contain continuous β-sheets with strands perpendicular to the fiber axis. Proteins commonly must undergo significant structural rearrangement to form cross β-fibers. Packed fibrils form twisted superhelical bundles that are probably the lowest energy folding state for many protein sequences. Indeed, cross β-patterns were first seen in the fiber diffraction pattern from denatured protein in boiled egg whites (Astbury et al., 1935).

The most detailed proposed model of a cross β-fibril, a four-stranded left-handed β-helix, is based on the diffraction pattern of ex vivo transthyretin fibrils (Blake & Serpell, 1996). A number of other fibers can be fit to the same model, with a repeat of 24 β-strands in 115.5 Å (Sunde et al., 1997). The well-ordered diffraction from $tau_{265–272}$, which bears the same overall characteristics as the less well-oriented patterns obtained for NFTs from Alzheimer's brain tissue (Kirschner et al., 1986), can be compared in detail to these earlier models. The $tau_{265–272}$ pattern best fits a model with a repeat distance slightly more than double that of the other fibers, but proposing a small difference in twist allows the data to be fit to virtually the same model (for a lucid discussion of the effect of small differences in pitch on fiber indexing, see Dickerson, 1964). The width of individual $tau_{265–272}$ fibrils estimated from diffraction data is 148 Å, compared to 64 Å fitted to fiber data for transthyretin (Blake & Serpell, 1996). This lateral dimension correlates well with the width of individual fibers from tau preparations as measured by electron microscopy (12–15 nm [120–150 Å]). The narrower transthyretin fibers are also narrower by electron microscopy, showing an average width of 8–10 nm (Coimbra & Andrade, 1971).

Implications for the folding and misfolding of tau

Fibers of full-length 4R tau did not have a cross β-structure, although the semicrystalline fiber diffraction pattern still suggests significant β-content. In other fiber forming diseases, there is a crucial region in the amyloidogenic protein that seems to be responsible for the formation of a cross β-fiber core (Booth et al., 1997; Inouye & Kirschner, 1997). Because the repeat region of tau forms the core of the fibers found in Alzheimer's disease brain (Wischik et al., 1988a, 1988b), a reasonable conjecture is that the repeat regions form a cross β-core while the rest of the tau polypeptide is excluded from the core. Perhaps a domain outside the core region prevents formation of a cross β-conformation in 4R tau. This conjecture is supported by the work of von Bergen et al. (2000). They found that a peptide with a sequence nearly identical to $tau_{265–272}$ formed fibrils much more slowly when it was embedded in a larger peptide. Another polypeptide with a sequence similar to $tau_{215–358}$ formed fibers 15 times faster than the full-length protein. They observed that fibers formed from full length tau 13 times faster in the presence of seeds consisting of of fibrils of repeat domain peptides.

One candidate for the region that can inhibit cross β-fiber formation is the proline-rich region, which is located to the N-terminal side of the microtubule binding domain. Functional studies show that the proline-rich region greatly enhances the binding and assembly activities of the microtubule binding domain, although it does not itself bind microtubules (Goode et al., 1997). It may reinforce a particular ordered structure in the repeat region. Another attractive hypothesis is that the N-terminal half of 4R tau may contain one or more separate domains whose folding must be disrupted to allow the formation of cross β-fibers.

Our results and those of von Bergen et al. suggest a possible mechanism for the accumulation of neurofibrillary tangles: C-terminal truncation (Mena et al., 1996) or other proteolysis of tau promotes the nucleation of PHF formation. For example, it may be necessary to remove a properly folded N-terminal tau domain before fiber growth can be nucleated. Full-length tau might only be able to add to existing cross β-fibers started with fragments. The recovery of soluble N-terminal fragments of tau from the cerebral-spinal fluid of Alzheimer's disease patients (Johnson et al., 1997) is consistent with this hypothesis. Another possibility is that the 4R tau fibers we have analyzed are intermediates on a pathway to the cross β-conformation. We think this possibility unlikely because classic fiber diffraction studies with silk showed the conversion from parallel β to cross β patterns to be a two state process (Rudall, 1962).

Soluble tau has shown little evidence of β-structure when analyzed by circular dichroism (Cleveland et al., 1977b; Schweers et al., 1994). An apparent lack of structure may be a consequence of the method of sample preparation. Alternatively, a β-conformation may be assumed by some sections of tau only during fiber assembly. Mutations in a tau fragment from the repeat region that were designed to reduce the ability to form β-sheets also reduced the ability to form fibers (Pérez et al., 1996). Similarly, the substitution of proline at various locations in fibrillogenic tau peptides disrupted their ability to form fibers (von Bergen et al., 2000). Our fiber diffraction analysis of repeat region peptides supports the general idea that β-sheet content is important to fiber formation. Additionally, the fiber pattern of full-length tau is consistent with β-structure content, although not aligned in a simple way either perpendicular or parallel to the fiber axis.

Nature of the fibers in tauopathic diseases

The diffraction pattern seen in PHF material isolated from affected brain suggested a cross β-pattern (Kirschner et al., 1986), but it has been argued that this pattern could have arisen from contaminating amyloid β-peptide (Schweers et al., 1994). In light of our data and the growing body of evidence linking amyloidogenic diseases to cross β-fibril formation, it seems more reasonable to believe the original interpretation is correct. Although some of the peptides we have studied are short, it is important to note that they can assume a cross β-conformation, and that in solution they possess inherent microtubule binding activity. These peptides, perhaps in or out of the context of the complete protein, may nucleate fiber assembly leading to PHF formation.

A formal possibility is that tau fibers from a variety of different tauopathic dementias may not all have the same molecular structure. Although it seems unlikely, our data do not rule out the possibility that fiber structure is dependent on tau isoform content. All six isoforms of tau have been reported to be present in Alzheimer's disease PHFs (Greenberg & Davies, 1990; Brion et al., 1991b; Lee et al., 1991; Goedert et al., 1992; Greenberg et al., 1992; Mulot et al., 1994). By contrast, only three repeat tau in its three isoforms is present in some cases identified as Pick's disease (Delacourte & Buée, 1997) while other well-defined familial tauopathies such as FTDP-17 are characterized by fibers made of only four repeat tau (Spillantini et al., 1997; Hutton et al., 1998). Other neurodegenerative diseases also vary in which tau isoforms are included in pathological fibers (reviewed, Spillantini et al., 1997; Delacourte et al., 1998). Fiber diffraction analysis of 3R tau would help resolve this issue, but we have not yet succeeded in growing fibers of 3R tau.

Our results call for caution in applying electron microscopy to determine the structure of pathological fibers or fibers assembled in vitro. Our four types of fibers are similar by electron microscopy despite the vast differences in size and composition of the constituent polypeptides. The gross appearance by electron microscopy is similar, even though X-ray diffraction reveals important differences in fiber structure. Conversely, what appear by microscopy to be major differences in fiber forms may reflect only minor differences in the fundamental structure of the fiber.

We suspect that full-length tau is capable of folding into a stable structure, and that misregulation or damage to that structure is key to the intracellular pathology of Alzheimer's disease and other tauopathies. We hope that increased understanding of tau's structural capabilities can provide clues regarding tau pathology.

Materials and methods

Peptide synthesis

The peptide amide from residues 265–272 (KVQIINKK) and the peptide amide from residues 247–272 (VRSKIGSTENLKHQPG GGKVQIINKK) were synthesized on a Millipore 9050 Plus peptide synthesizer by DIPCDI/HoBT chemistry (Millipore Corp., Bedford, Massachusetts). Following cleavage and deprotection (Solé & Barany, 1992), peptides were purified to >99% by reversed-phase HPLC, lyophilized, and resuspended in buffer (20 mM HEPES, pH 6.8). Peptide integrity was confirmed by fast atomic bombardment mass spectrometry.

Protein purification

Four repeat *Rattus norvegicus* tau containing both N-terminal inserts (4R tau) was expressed in BL21 cells using the pET expression system of Novagen (Madison, Wisconsin) as described previously (Kosik et al., 1989; Goode & Feinstein, 1994). Protein production was induced with 1 mM IPTG, and bacterial cells were harvested by centrifugation; the pellets were stored at −70 °C until use. The cells were resuspended in tau buffer (50 mM Tris pH 7.6 at 21 °C, 25 mM NaCl, 10% v/v glycerol, 2 mM dithiothreitol) with 0.1 mM phenylmethylsulfonylfluoride and lysed by passage through a French pressure cell. All purification steps were at 4 °C. After centrifugation (28,000 × *g*, 30 min) the supernatant was passed over a DEAE cellulose column (DE-52, Whatman) equilibrated in the tau buffer. Fractions were analyzed by SDS polyacrylamide gel electrophoresis (Laemmli, 1970). Fractions enriched in tau were combined and loaded on a phosphocellulose column (P-11, Whatman, Clifton, New Jersey) equilibrated in tau buffer with 100 mM NaCl. Tau was eluted with a linear gradient of 100–400 mM NaCl. Fractions enriched in tau were combined, and $(NH_4)_2SO_4$ and tris (2-carboxyethyl)-phosphinehydrochloride (TCEP, Boehringer Mannheim, Germany) were added to 500 and 1 mM, respectively. This sample was loaded on an octyl sepharose column (Pharmacia, Uppsala, Sweden) and a gradient was run from 500 mM to zero $(NH_4)_2SO_4$, followed by additional washing in the absence of $(NH_4)_2SO_4$. Tau, which eluted during the zero $(NH_4)_2SO_4$ wash, was precipitated by addition of $(NH_4)_2SO_4$ to 70% of saturation, and was then resuspended in a minimum volume of tau buffer. After a second round of precipitation with $(NH_4)_2SO_4$, purified concentrated tau was resuspended and dialyzed against tau buffer. Final protein concentration was about 15 mg/mL (330 μM) with a yield of about 2 mg protein per gram of starting cell pellet. The sample appeared homogenous by SDS polyacrylamide gel electrophoresis. The purified final sample was shown to assemble microtubules.

$Tau_{215–358}$ was expressed as described for 4R tau (above). *Escherichia coli* cells containing tau were lysed by sonication in a buffer containing 20 mM NaCl, 50 mM tris, pH 8.0. The supernatant from the lysis was made 4% (v/v) trifluoroacetic acid, the resulting pellet was removed by centrifugation, and the tau containing supernatant was neutralized by addition of concentrated tris, pH 8.0. $Tau_{215–358}$ was then purified to homogeneity by reversed-phase HPLC on a 300 Å pore size C18 column using an isopropanol gradient with 0.1% trifluoroacetic acid as a counterion.

Fiber preparation

Fibers were grown by hanging drop vapor diffusion. Two microliter samples of protein or peptide were mixed with an equal volume of a solution designed to precipitate the sample. These 4 μL drops were suspended over a 1 mL reservoir of the precipitating solution and allowed to equilibrate. Within a few days macroscopic fibers of the two synthetic peptides appeared in the drops. 4R tau and $tau_{215–358}$ fibers took several weeks to grow.

4R tau fibers were grown at 17 °C at 12 mg/mL protein over well solutions containing 50 mM sodium acetate pH 4.7, 50 mM calcium chloride, 10% v/v glycerol, 0.02% w/v sodium azide, and 18–28% 2-methyl-2,4-pentanediol. The fiber of $tau_{215–358}$ was grown at room temperature at 8 mg/mL protein with a well solution containing 30% PEG 5000, 0.2 M $MgCl_2$, 50 mM tris pH 8.5; the drops also contained an equimolar concentration of a peptide corresponding to amino acids 410–445 of human β4 tubulin, but no tubulin peptide was detected in the fibers. Fibers of the $tau_{247–272}$

peptide were grown at 17 °C from a 25 mg/mL peptide solution and 30% w/v PEG 8000, 0.2 M $(NH_4)_2SO_4$, 50 mM HEPES, pH 7.5. Fibers of the $tau_{265–272}$ peptide were grown at room temperature from a 10 mg/mL peptide solution and a precipitating solution containing 28% w/v PEG 8000 and 1.5 M Li_2SO_4, pH 7.0.

Fiber diffraction

Fibers were harvested and stored by methods similar to those commonly used for protein crystals. Storage solutions contained all the components of the vapor diffusion experiment with the concentration of the precipitating agent slightly increased. Individual fibers were mounted in glass capillaries with their long axis roughly parallel to the long axis of the capillary and sealed in an atmosphere saturated with storage solution vapor. Diffraction data were collected at room temperature on a Rigaku RU-200 generator operating at 50 kV, 100 mA equipped with a copper anode and a mirror focusing system. Images were recorded using an R-axis IIc image plate detector. Exposure time was 40, 20, 20, or 10 min for the $tau_{265–272}$, $tau_{247–272}$, $tau_{215–358}$, or 4R tau fibers, respectively.

Electron microscopy

The mother liquor from the drops that had macroscopic fibers removed for X-ray analysis was used as the source of material for microscopy. The liquid was applied directly to formvar-coated copper grids, which were then stained with uranyl acetate. A Philips CM10 electron microscope was used at 80 kV.

Supplementary material in the Electronic Appendix

Model of a cross β-fibril based on the helical parameters derived from $tau_{265–272}$ fibers (KVQIINKK). Interstrand spacing is 4.7 Å and intersheet spacing 10.6 Å. The handedness of the helix and the direction of the strands (parallel or antiparallel) cannot be resolved with fiber diffraction data and is shown left handed and parallel by the convention of Blake and Serpell (1996). This model predicts a hydrophobic core composed of the peptide's dileucine motif and a hydrogen bonded ladder running the length of the helix and composed of asparagine and glutamine residues. Model built in Insight95 (Biosym, San Diego, California) and extended with Moleman (Kleywegt & Jones, 1997). Figure generated with MOLSCRIPT (Kraulis, 1991) and rendered with Raster3D (Merritt & Murphy, 1994).

Acknowledgments

We thank R.E. Marsh and D.C. Rees for helpful comments on our data and models. Kenneth Linberg provided valuable help with figures. This work was supported by the Sigma Kappa Foundation Alzheimer's and Gerontology Related Research Grant Program, by the Alzheimer's Association/Mr. and Mrs. Carroll O'Connor Pilot Research Grant # PRG-94-031, and by NINDS Grant #1 RO1 NS35010-01. L.A.K. was an American Cancer Society Junior Faculty Fellow (JFRA-572). M.-F.C. was the recipient of PHS #1 F32 NS 10212-0 postdoctoral fellowship. A.M.G. was supported by an REU supplement to NSF Grant #MCB-9505977; a fellowship from the Center for Quantized Electronic Structures (QUEST), an NSF Science and Technology Center, #DMR 91-20007; and by a Howard Hughes Medical Institute undergraduate fellowship.

References

Arrasate M, Perez M, Valpuesta JM, Avila J. 1997. Role of glycosaminoglycans in determining the helicity of paired helical filaments. *Am J Pathol 151*: 1115–1122.

Astbury WT, Dickinson S, Bailey K. 1935. The X-ray interpretation of denaturation and the structure of the seed globulins. *Biochem J 29*:2351–2360.

Black MM, Slaughter T, Moshiach S, Obrocka M, Fischer I. 1996. Tau is enriched on dynamic microtubules in the distal region of growing axons. *J Neurosci 16*:3601–3619.

Blake C, Serpell L. 1996. Synchrotron X-ray studies suggest that the core of the transthyretin amyloid fibril is a continuous beta-sheet helix. *Structure 4*:989–998.

Binder LI, Frankfurter A, Rebhun LI. 1985. The distribution of tau in the mammalian central nervous system. *J Cell Biol 101*:1371–1378.

Booth DR, Sunde M, Bellotti V, Robinson CV, Hutchinson WL, Fraser PE, Hawkins PN, Dobson CM, Radford SE, Blake CC, et al. 1997. Instability, unfolding and aggregation of human lysozyme variants underlying amyloid fibrillogenesis. *Nature 385*:787–793.

Bouras C, Giannakopoulos P, Good PF, Hsu A, Hof PR, Perl DP. 1997. A laser microprobe mass analysis of brain aluminum and iron in dementia pugilistica: Comparison with Alzheimer's disease. *Eur Neurol 38*:53–58.

Brion JP, Hanger DP, Bruce MT, Couck AM, Flament-Durand J, Anderton BH. 1991a. Tau in Alzheimer neurofibrillary tangles. N- and C-terminal regions are differentially associated with paired helical filaments and the location of a putative abnormal phosphorylation site. *Biochem J 273*:127–133.

Brion JP, Hanger DP, Couck AM, Anderton BH. 1991b. A68 proteins in Alzheimer's disease are composed of several tau isoforms in a phosphorylated state which affects their electrophoretic mobilities. *Biochem J 279*:831–836.

Brion JP, Passareiro H, Nunez J, Flament-Durand J. 1985. Mise en evidence immunologique de la proteine tau au niveau des lesions de degenerescence neurofibrillaire de la maladie d'Alzheimer. *Arch Biol 95*:229–235.

Burge RE. 1963. Equatorial X-ray diffraction by fibrous proteins: Short-range order in collagen, feather keratin and F-actin. *J Mol Biol 7*:213–224.

Butner KA, Kirschner MW. 1991. Tau protein binds to microtubules through a flexible array of distributed weak sites. *J Cell Biol 115*:717–730.

Caceres A, Kosik KS. 1990. Inhibition of neurite polarity by tau antisense oligonucleotides in primary cerebellar neurons. *Nature 343*:461–463.

Cleveland DW, Hwo S-Y, Kirschner MW. 1977a. Purification of tau, a microtubule-associated protein that induces assembly of microtubules from purified tubulin. *J Mol Biol 116*:207–225.

Cleveland DW, Hwo SY, Kirschner MW. 1977b. Physical and chemical properties of purified tau factor and the role of tau in microtubule assembly. *J Mol Biol 116*:227–247.

Coimbra A, Andrade C. 1971. Familial amyloid polyneuropathy: An electron microscope study of the peripheral nerve in five cases. I. Interstitial changes. *Brain 94*:199–206.

Crowther RA, Oleson OF, Jakes R, Goedert M. 1992. The microtubule binding repeats of tau protein assemble into filaments like those found in Alzheimer's disease. *FEBS Lett 309*:199–202.

Crowther RA, Oleson OF, Smith MJ, Jakes R, Goedert M. 1994. Assembly of Alzheimer-like filaments from full-length tau protein. *FEBS Lett 337*:135–138.

Crowther RA, Wischik CM. 1985. Image reconstruction of the Alzheimer paired helical filament. *EMBO J* 4:3661–3665.

Delacourte A, Buée L. 1997. Normal and pathological tau proteins as factors for microtubule asembly. *Int Rev Cytol 171*:167–224.

Delacourte A, Sergeant N, Wattez A, Gauvreau D, Robitaille Y. 1998. Vulnerable neuronal subsets in Alzheimer's and Pick's disease are distinguished by their τ isoform distribution and phosphorylation. *Ann Neurol 43*:193–204.

Dickerson RE. 1964. X-ray analysis and protein structure. In: Neurath H, ed. *The proteins*, 2nd ed., vol. 2. New York: Academic Press. pp 603-778.

Drechsel DN, Hyman AA, Cobb MH, Kirschner MW. 1992. Modulation of the dynamic instability of tubulin assembly by the microtubule-associated protein tau. *Mol Biol Cell 3*:1141–1154.

Eanes ED, Glenner GG. 1968. X-ray diffraction studies of amyloid filaments. *J Histochem Cytochem 16*:673–677.

Ennulat DJ, Liem RKH, Hashim GA, Shelanski ML. 1989. Two separate 18-amino acid domains of tau promote the polymerization of tubulin. *J Biol Chem 264*:5327–5330.

Feany MB, Dickson DW. 1996. Neurodegenerative disorders with extensive tau pathology: A comparative study and review. *Ann Neurol 40*:139–148.

Fellous A, Francon J, Lennon AM, Nunez J. 1976. Initiation of neurotubulin polymerisation and rat brain development. *FEBS Lett 64*:400–403.

Goedert M, Jakes R, Spillantini MG, Hasegawa R, Smith MJ, Crowther RA. 1996a. Assembly of microtubule associated protein tau into Alzheimer-like filaments induced by sulphated glycosaminoglycans. *Nature 383*:550–553.

Goedert M, Spillantini MG, Cairns NJ, Crowther RA. 1992. Tau proteins of Alzheimer paired helical filaments: Abnormal phosphorylation of all six brain isoforms. *Neuron 8*:159–168.

Goedert M, Spillantini MG, Hasegawa R, Jakes R, Crowther RA, Klug A. 1996b. Molecular dissection of the neurofibrillary lesions of Alzheimer's disease. *Cold Spring Harbor Symp Quant Biol 61*:565–573.

Goedert M, Wischik CM, Crowther RA, Walker JE, Klug A. 1988. Cloning and sequencing of the cDNA encoding a core protein of the paired helical filament of Alzheimer disease: Identification as the microtubule-associated protein tau. *Proc Natl Acad Sci USA 85*:4051–4055.

Goode BL, Denis PE, Panda D, Radeke MJ, Miller HP, Wilson L, Feinstein SC. 1997. Functional interactions between the proline-rich and repeat regions of tau enhance microtubule binding and assembly. *Mol Biol Cell 8*:353–365.

Goode BL, Feinstein SC. 1994. Identification of a novel microtubule binding and assembly domain in the developmentally regulated inter-repeat region of tau. *J Cell Biol 124*:769–782.

Greenberg SG, Davies P. 1990. A preparation of Alzheimer paired helical filaments that displays distinct tau proteins by polyacrylamide gel electrophoresis. *Proc Natl Acad Sci USA 87*:5827–5831.

Greenberg SG, Davies P, Schein JD, Binder LI. 1992. Hydrofluoric acid-treated tau PHF proteins display the same biochemical properties as normal tau. *J Biol Chem 267*:564–569.

Grundke-Iqbal I, Iqbal K, Quinlan M, Tung Y-C, Zaidi MS, Wisniewski HM. 1986. Microtubule associated protein tau: A component of Alzheimer paired helical filaments. *J Biol Chem 261*:6084–6089.

Gustke N, Trinczek B, Biernat J, Mandelkow EM, Mandelkow E. 1994. Domains of tau protein and interactions with microtubules. *Biochemistry 33*:9511–9522.

Hutton M, Lendon CL, Rizzu P, Baker M, Froelich S, Houlden H, Pickering-Brown S, Chakraverty S, Isaacs A, Grover A, et al. 1998. Association of missense and 5′ splice-site mutations in tau with the inherited dementia FTDP-17. *Nature 393*:702–705.

Inouye H, Kirschner DA. 1997. X-ray diffraction analysis of scrapie prion: Intermediate and folded structures in a peptide containing two putative alpha-helices. *J Mol Biol 268*:375–389.

Jakes R, Novak M, Davison M, Wischik CM. 1991. Identification of 3- and 4-repeat tau isoforms within the PHF in Alzheimer's disease. *EMBO J 10*:2725–2729.

Johnson GV, Seubert P, Cox TM, Motter R, Brown JP, Galasko D. 1997. The tau protein in human cerebrospinal fluid in Alzheimer's disease consists of proteolytically derived fragments. *J Neurochem 68*:430–433.

Kelly JW. 1996. Alternative conformations of amyloidogenic proteins govern their behavior. *Curr Opin Struct Biol 6*:11–17.

Kirschner DA, Abraham C, Selkoe DJ. 1986. X-ray diffraction from intraneuronal paired helical filaments and extraneuronal amyloid fibers in Alzheimer disease indicates cross-β conformation. *Proc Natl Acad Sci USA 83*:503–507.

Kleywegt GJ, Jones TA. 1997. Model-building and refinement practice. *Methods Enzymol 277*:208–230.

Kondo J, Honda T, Mori H, Hamada Y, Miura R, Ogawara M, Ihara Y. 1988. The carboxyl third of tau is tightly bound to paired helical filaments. *Neuron 1*:827–834.

Kosik KS, Joachim CL, Selkoe DJ. 1986. Microtubule-associated protein tau (τ) is a major antigenic component of paired helical filaments in Alzheimer disease. *Proc Natl Acad Sci USA 83*:4044–4048.

Kosik KS, Orecchio LD, Bakalis S, Neve RL. 1989. Developmentally regulated expression of specific tau sequences. *Neuron 2*:1389–1397.

Kraulis PJ. 1991. MOLSCRIPT: A program to produce both detailed and schematic plots of protein structures. *J Appl Crystallogr 24*:946–950.

Ksiezak-Reding H, Shafit-Zagardo B, Yen S-H. 1995. Differential expression of exons 10 and 11 in normal tau and tau associated with paired helical filaments. *J Neurosci Res 41*:583–593.

Ksiezak-Reding H, Yen SH. 1991. Structural stability of paired helical filaments requires microtubule-binding domains of tau: A model for self-association. *Neuron 6*:717–728.

Laemmli UK. 1970. Cleavage of structural proteins during the assembly of the head of bacteriophage T4. *Nature 227*:680–685.

Lee G, Cowan N, Kirschner MW. 1988. The primary structure and heterogeneity of tau protein from mouse brain. *Science 239*:285–288.

Lee G, Neve RL, Kosik KS. 1989. The microtubule binding domain of tau protein. *Neuron 2*:1615–1624.

Lee VM, Balin BJ, Otvos L Jr, Trojanowski JQ. 1991. A68: A major subunit of paired helical filaments and derivatized forms of normal tau. *Science 251*:675–678.

Lindwall G, Cole RD. 1984. The purification of tau protein and the occurrence of two phosphorylation states of tau in brain. *J Biol Chem 259*:12241–12245.

Malinchik SB, Inouye H, Szumowski KE, Kirschner DA. 1998. Structural analysis of Alzheimer's beta(1–40) amyloid: Protofilament assembly of tubular fibrils. *Biophys J 74*:537–545.

Marsh RE, Corey RB, Pauling L. 1955. An investigation of the structure of silk fibron. *Biochim Biophys Acta 16*:1–35.

Mena R, Edwards PC, Harrington CR, Mukaetova-Ladinska EB, Wischik CM. 1996. Staging the pathological assembly of truncated tau protein into paired helical filaments in Alzheimer's disease. *Acta Neuropathol 91*:633–641.

Merritt EA, Murphy MEP. 1994. Raster3D Version 2.0, a program for Photorealistic molecular graphics. *Acta Crystallogr D 50*:869–873.

Montejo de Garcini E, Carrascosa JL, Correas I, Nieto A, Avila J. 1988. Tau factor polymers are similar to paired helical filaments of Alzheimer's disease. *FEBS Lett 236*:150–154.

Mulot SF, Hughes K, Woodgett JR, Anderton BH, Hanger DP. 1994. PHF-tau from Alzheimer's brain comprises four species on SDS-PAGE which can be mimicked by in vitro phosphorylation of human brain tau by glycogen synthase kinase-3 beta. *FEBS Lett 349*:359–364.

Novak M, Kabat J, Wischik CM. 1993. Molecular characterization of the minimal protease resistant tau unit of the Alzheimer's disease paired helical filament. *EMBO J 12*:365–370.

Panda D, Goode BL, Feinstein SC, Wilson L. 1995. Kinetic stabilization of microtubule dynamics at steady state by tau and microtubule-binding domains of tau. *Biochemistry 34*:11117–11127.

Pauling L, Corey R. 1951. Configuration of polypeptide chains with favored orientation around single bonds: Two new pleated sheets. *Proc Natl Acad Sci USA 37*:729–739.

Pérez M, Valpuesta JM, Medina M, Montejo de Garcini E, Avila J. 1996. Polymerization of τ into filaments in the presence of heparin: The minimal sequence required for τ-τ interaction. *J Neurochem 67*:1183–1190.

Reed LA, Grabowski TJ, Schmidt ML, Morris JC, Goate A, Solodkin A, Van Hoesen GW, Schelper RL, Talbot CJ, Wragg MA, et al. 1997. Autosomal dominant dementia with widespread neurofibrillary tangles. *Ann Neurol 42*:564–572.

Ruben GC, Iqbal K, Wisniewski HM, Johnson JE Jr, Grundke-Iqbal I. 1992. Alzheimer neurofibrillary tangles contain 2.1 nm filaments structurally identical to the microtubule associated protein T: A high resolution transmission electron microscope study of tangles and senile plaque core amyloid. *Brain Res 590*:164–179.

Rudall KM. 1962. *Silk and other cocoon proteins.* In: Florkin M, Mason HS, eds. *Comparative biochemistry: A comprehensive treatise*, vol. IV. New York: Academic Press. p 397.

Schweers O, Mandelkow EM, Biernat J, Mandelkow E. 1995. Oxidation of cys-322 in the repeat domain of microtubule-associated protein tau controls the in vitro assembly of paired helical filaments. *Proc Natl Acad Sci USA 92*:8463–8467.

Schweers O, Schonnbrun-Hanebeck E, Marx A, Mandelkow E. 1994. Structural studies of tau protein and Alzheimer paired helical filaments show no evidence for β-structure. *J Biol Chem 269*:24290–24297.

Solé NA, Barany G. 1992. Optimization of solid-phase synthesis of [ala8]-dynorphin-A. *J Org Chem 57*:5399–5403.

Spillantini MG, Goedert M, Crowther RA, Murrell JR, Farlow MR, Ghetti B. 1997. Familial multiple system tauopathy with presenile dementia: A disease with abundant neuronal and glial tau filaments. *Proc Natl Acad Sci USA 94*:4113–4118.

Spillantini MG, Murrell JR, Goedert M, Farlow MR, Klug A, Ghetti B. 1998. Mutation in the tau gene in familial multiple system tauopathy with presenile dementia. *Proc Natl Acad Sci USA 95*:7737–7741.

Sunde M, Serpell LC, Bartlam M, Fraser PE, Pepys MB, Blake CF. 1997. Common core structure of amyloid fibrils by synchrotron X-ray diffraction. *J Mol Biol 273*:729–739.

Trojanowski JQ, Lee VMY. 1998. Aggregation of neurofilament and alpha-synuclein proteins in Lewy bodies: Implications for the pathogenesis of Parkinson disease and Lewy body dementia. *Arch Neurol 55*:151–152.

von Bergen M, Friedhoff P, Biernat J, Heberle J, Mandelkow EM, Mandelkow E. 2000. Assembly of tau protein into Alzheimer paired helical filaments depends on a local sequence motif ((306)VQIVYK(311)) forming beta structure. *Proc Natl Acad Sci USA 97*:5129–5134.

Weingarten MD, Lockwood AH, Hwo S-Y, Kirschner MW. 1975. A protein factor essential for microtubule assembly. *Proc Natl Acad Sci USA 72*:1858–1862.

Wischik CM, Crowther RA, Stewart M, Roth M. 1985. Subunit structure of paired helical filaments in Alzheimer's disease. *J Cell Biol 100*:1905–1912.

Wischik CM, Novak M, Edwards PC, Klug A, Tichelaar W, Crowther RA. 1988a. Structural characterization of the core of the paired helical filament of Alzheimer disease. *Proc Natl Acad Sci USA 85*:4884–4888.

Wischik CM, Novak M, Thøgerson HC, Edwards PC, Runswick MJ, Jakes R, Walker JE, Milstein C, Roth M, Klug A. 1988b. Isolation of a fragment of tau derived from the core of the paired helical filament of Alzheimer disease. *Proc Natl Acad Sci USA 85*:4506–4510.

Wood JG, Mirra SS, Pollock NJ, Binder LI. 1986. Neurofibrillary tangles of Alzheimer disease share antigenic determinants with the axonal microtubule-associated protein tau (τ). *Proc Natl Acad Sci USA 83*:4040–4043.

Yanagawa H, Chung SH, Ogawa Y, Sato K, Shibata-Seki T, Masai J, Ishiguro K. 1998. Protein anatomy: C-tail region of human tau protein as a crucial structural element in Alzheimer's paired helical filament formation in vitro. *Biochemistry 37*:1979–1988.